University of Birjand

Water Harvesting Research Vol. 8, No. 1, Spring & Summer 2025, Original paper p. 105-122

10.22077/JWHR.2025.9149.1174

Remote Sensing and Machine Learning for Groundwater Spring Potential Assessment in Eastern and Northeastern Iran

Javad Momeni Damaneh[a], Samira Gerami[b&*], Mahboobeh Hajibigloo[c]

[a]Department of Natural Resources Engineering, Agriculture and Natural Resources Faculty, Hormozgan University, Bandarabbas, Iran
[b]Department of Civil Engineering, University of Birjand, Birjand, Iran
[c]Department of Natural Resources Engineering, Agriculture and Natural Resources Faculty, Gorgan University, Gorgan, Iran

[*]Corresponding Author, E-mail address: samiragerami9397@yahoo.com
Received: 05 April 2025/ **Revised**: 15 June 2025/ **Accepted**: 15 June 2025

Abstract

Groundwater (GW) resources are being over-exploited in many parts of the world due to the increasing demand for water driven by population growth and industrialization. This study addresses the critical need for assessing GW potential for sustainability, focusing on eastern and northeastern Iran. This research leverages a comprehensive analysis of environmental variables using advanced machine learning algorithms to model spring potential in this specific area. Sixty-six environmental variables were analyzed, including physiographic, climatic, soil, geological, vegetation cover, and hydrological factors. Various machine learning models, such as GLM, GBM, CTA, ANN, SRE, FDA, MARS, RF, MaxEnt, and ESMs were employed. Model accuracy was evaluated using KAPPA, TSS, and ROC indices, with 70% of the data used for training and 30% for evaluation through five repetitions. The findings indicated that Random Forest (RF) model achieved the highest accuracy based on the evaluation criteria. Relative importance analysis revealed that topographic factors (Altitude, TWI, Slope), climatic factors (BIO7, BIO19, BIO12), and soil factors (Sand 60-100 cm, Silt 60-100 cm, Clay 0-5 cm, Land Surface Temperature) were the most influential in predicting spring potential. The RF and Ensemble (ESMs) models identified 13.04% to 15.07% of the study area as having high to very high groundwater potential. The high performance of RF model and the identified key influencing factors provide valuable insights for sustainable water resource management in this data-scarce region. The findings underscore the utility of remote sensing-derived variables and machine learning for groundwater assessment and offer a practical GWPM for governmental and private sector use.

Keywords: Environmental Variables, Random Forest Algorithm, Water Resource Management, Spatial Modeling, Model Evaluation Metrics

1. Introduction

Globally, approximately 2.5 billion people rely on groundwater for their domestic water needs (Grönwall and Danert, 2020). The significance of these resources is projected to increase due to evolving climate conditions, including reduced rainfall and a heightened risk of severe droughts (Arneth et al., 2019). Groundwater constitutes about 34% of the world's freshwater reserves (Tariq et al., 2022) and serves as a critical source for meeting the needs of 97% of the global population and supporting 50% of worldwide irrigation (Tariq and Shu, 2020). Its widespread utilization spans domestic, industrial, and agricultural sectors across diverse regions (Mumtaz et al., 2023).

The development of a Groundwater Potential Map (GPM) is recognized as a vital tool for the effective planning and exploration of groundwater resources (Elbeih, 2015). However, a universally accepted definition of groundwater potential remains elusive. Consequently, GPM can encompass various approaches, including the development of spatial estimates of groundwater storage

within a specific area, the assessment of the likelihood of encountering groundwater, or the prediction of locations where the highest yield is anticipated (Díaz-Alcaide and Martínez-Santos, 2019).

Two primary methodologies exist for generating GPMs: expert opinion-based decision systems and machine learning methods. Expert opinion-based techniques, with a long history of application (DEP, 1993), include influential multi-factor approaches (Magesh et al., 2012; Nasir et al., 2018; Martín-Loeches et al., 2018), hierarchical analytical processes (Mohammadi-Behzad et al., 2019; Al-Djazouli et al., 2021), and Dempster-Shafer models (Mogaji and Lim, 2018; Obeidavi et al., 2021). These methods typically involve evaluating the weighting of environmental factors and analyzing their frequency ratios (Falah and Zeinivand, 2019; Boughariou et al., 2021).

In contrast, machine learning represents a relatively more recent approach. The fundamental distinction lies in machine learning's utilization of artificial intelligence to identify intricate relationships among significant environmental variables, making it particularly well-suited for mapping the potential of complex variables with numerous contributing factors, such as groundwater. Research in GPM highlights the application of various supervised classification methods. For instance, Al-Fugara and his team (2020) employed ensemble analysis for mapping spring potential in the Jordan watershed, while Odzemir (2011) utilized logistic regression to delineate spring potential in Turkey. Random forests are also widely adopted for mapping groundwater potential in diverse settings, ranging from mountainous aquifers (Moghaddam et al., 2020) to large alluvial basins (Martínez-Santos and Renard, 2020).

Other supervised classification techniques employed in GPM include boosted regression trees (Naghibi et al., 2016), support vector machines (Naghibi et al., 2017a), neural networks (Lee et al., 2012; Panahi et al., 2020), and ensemble methods (Naghibi et al., 2017b; Martínez-Santos and Renard, 2020; Nguyen et al., 2020b). Support Vector Machines (SVM), in particular, are commonly used for predicting potential groundwater zones (GWPZ), as demonstrated by Eid et al. (2023).

Groundwater Potential Mapping (GPM) operates on the principle that groundwater occurrence can be inferred from surface features of the earth. Common explanatory variables in GPM studies encompass geology, geological lines, landform, topography, soil, land use/land cover, drainage-related variables, slope, precipitation, and vegetation cover indices (Jha et al., 2007). Supervised classification algorithms are trained to identify correlations between these variables and known groundwater data.

When these algorithms yield accurate predictions, their results are extrapolated to estimate groundwater potential across a given study area. The capacity of artificial intelligence models to process substantial amounts of data and generate precise predictions has led to a recent surge in their application within water management (Yu et al., 2022; Masoudi et al., 2023).

Most Groundwater Potential Mapping (GPM) studies utilizing machine learning techniques encounter two primary challenges. The first is the limited availability of data for training and testing algorithms, coupled with the potentially large number of environmental variables. This underscores the necessity for precise categorization of these variables to minimize errors within the dataset. The second challenge lies in the evaluation of machine learning outcomes, which often relies on standard big data metrics such as accuracy, recall, and area under the curve (Pradhan, 2013; Naghibi et al., 2016; Chen et al., 2019).

While useful, standard evaluation metrics may have limited applicability in modeling scenarios where the input dataset consists solely of error-free samples. Furthermore, questions arise regarding the accuracy with which these metrics (presence points) represent presence data when developing spatially distributed estimations. In certain instances, the incorporation of temporary calibration elements, such as supplementary information from presence data, can facilitate a more accurate interpretation of the results (Martínez-Santos et al., 2021a).

A significant number of researchers have applied various probabilistic methods, including frequency ratio, analytic hierarchy process, logistic regression, evidence weight, Shannon entropy, and evidential belief

function, among other exploratory techniques, to delineate Groundwater Potential Zones (GWPZ) and groundwater recharge areas (Srivastava and Bhattacharya, 2006; Arthur et al., 2007; Ghayoumian et al., 2007; Chowdhury et al., 2008; Corsini et al., 2009; Murthy and Mamo, 2009; Chenini et al., 2010; Gupta and Srivastava, 2010; Oh et al., 2011; Ozdemir, 2011; Lee et al., 2012; Nampak et al., 2014; Pourtaghi and Pourghasemi, 2014; Moghaddam et al., 2015; Naghibi et al., 2016; Devanantham et al., 2020; Kamali et al., 2020; Al-Kindi et al., 2022; Bhadani et al., 2023; AlAyyash et al., 2023; Singh et al., 2018; Shah et al., 2021; Seifu et al., 2023).

Given the extensive existing research on groundwater potential mapping (GPM) utilizing machine learning and remote sensing techniques, the present study distinguishes itself through several key aspects: it employs a comprehensive analysis of 66 key environmental variables, encompassing a wider range of influential parameters than many preceding studies; it focuses specifically on the eastern and northeastern regions of Iran, characterized by unique climatic and ecological features, and utilizes a substantial dataset of 7,355 officially recorded active spring locations, enabling the development of a more accurate and effective model and map for this particular area; it systematically compares the performance of ten advanced machine learning algorithms from the Biomod2 software package to identify the optimal algorithm for the study region.

It emphasizes the importance of remote sensing (RS)-derived variables as a valuable source of information, particularly in areas with limited access to conventional data, to produce a practical groundwater potential map (GWPM) for governmental and private sector use in the assessment, management, and conservation of water resources in eastern and northeastern Iran. This study underscores the significance of comprehensive variable selection, precise geographic focus, a robust presence dataset, algorithmic comparison, and the role of remote sensing in promoting sustainable water resource management within this region.

2. Materials and Methods

2.1. Study area

The present study was carried out in the eastern and northeastern regions of Iran, covering a total area of 295,115 square kilometers. The geographical coordinates of the study area range between longitudes 36° 26' 55" to 34° 26' 61" and latitudes 54° 31' 30" to 53° 11' 38". For a visual overview of the study area, refer to Figure 1. This region falls within the Iranian-Turanian phytogeographical zone, characterized by extensive natural diversity and unique ecological features in each sub-region Based on the Köppen climate classification, the region primarily experiences a cold arid climate, with some parts classified as cold semi-arid. The average annual precipitation is approximately 209.8 millimeters, though its distribution is uneven, generally decreasing from north to south. Precipitation ranges from a minimum of 116.2 millimeters to a maximum of 312.8 millimeters. In terms of temperature, the province's minimum recorded temperature is 12.2°C, while the maximum is 18.2°C, with an average annual temperature of 15.6°C (Damaneh et al., 2022).

The study area consists of 2,482 plant species across 585 genera and 115 families. The Asteraceae family is the most represented, with 303 species, followed by the Poaceae family with 180 species and the Lamiaceae family with 122 species. Notable plants in the region include Gav, Kolah Mirhossein, Choobak, Ashnian, Aspers, Ars, Baneh, Gaz, Barberry, and the Iranian rose. However, several valuable edible and medicinal plants, such as Anise, Thyme, Cumin, and Basil, are under threat of extinction due to overgrazing and rangeland degradation.

2.2. Determination of groundwater spring presence points

The active spring locations were determined using data provided by the Water Organization of Khorasan Province (Northern, Razavi, Southern). To represent absence locations, 2,000 random points were selected from the background. Overall, 7,355 active spring locations were recorded, officially registered by the regional water company using Global Positioning System (GPS) technology as depicted in Figure 1.

2.3. Determination of environmental variables

A review of previous studies, regional spring types, and available baseline data led to the identification of 66 key variables that influence the distribution and identification of potential spring areas. These variable layers were compiled from various sources.

A total of 66 environmental variables were utilized for model generation, comprising 6 physiographic variables, 24 climatic variables, 29 soil variables, 3 geological variables, 2 vegetation cover variables, and 2 hydrological variables. The modeling process is illustrated in Figure 2. Since all input layers of the model must have the same reference system, coordinate system, and scale, the preprocessing and initial processing of the information layers were performed using Idrisi Selva software (Damaneh et al., 2022).

The preparation of information layers and synchronization of layers with a pixel size of 1000*1000 meters in Idrisi Selva software were carried out utilizing a Pearson correlation coefficient of 0.8. Figure 3 illustrates the Pearson correlation test results of 66 predictors. Negative correlations are shown in red, while positive correlations are depicted in blue. The intensity of the color and the size of the circle represent the magnitude of the correlation coefficients. Variables with a correlation below 80% were selected (Zhang et al., 2021; Damaneh et al., 2022).

Table 1 presents the predictive variables utilized in modeling areas with homogeneous potential for spring presence. As shown in Table 1, Finally, 34 environmental parameters were selected as predictor variables and formatted as a Grid, along with the target spring presence points, for modeling in R software.

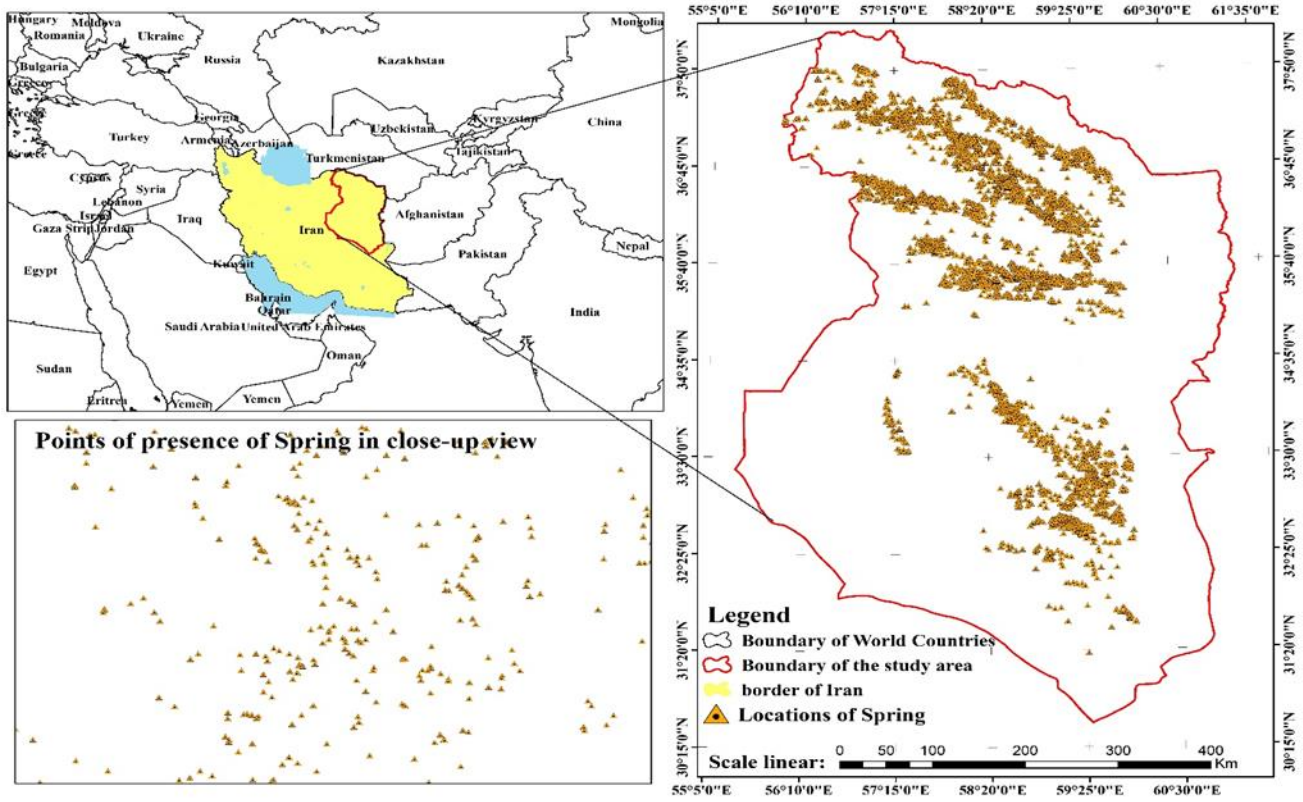

Fig. 1. Geographical location of the study area and distribution of natural spring presence points in eastern and northeastern Iran

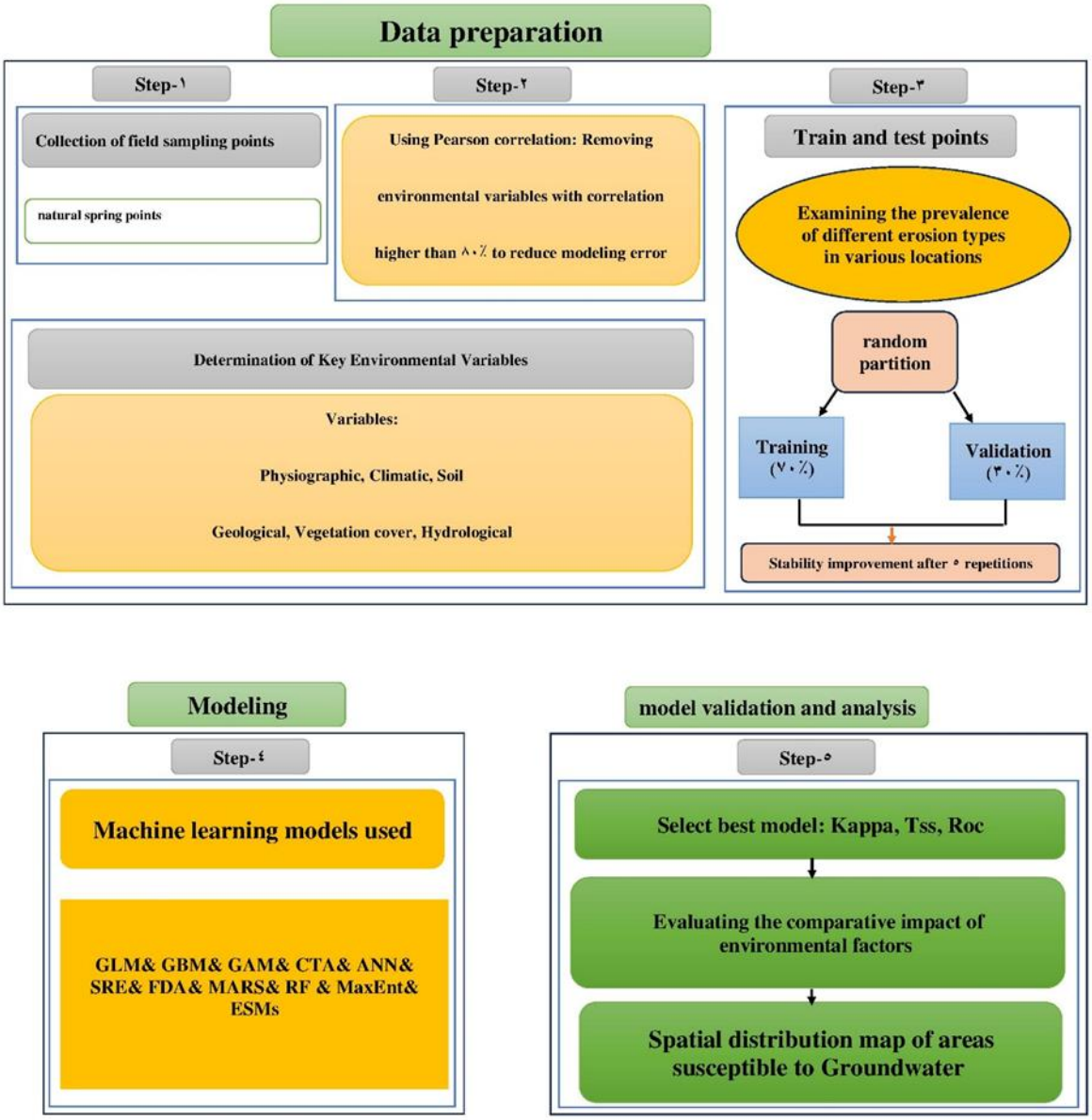

Fig. 2. The process of modeling

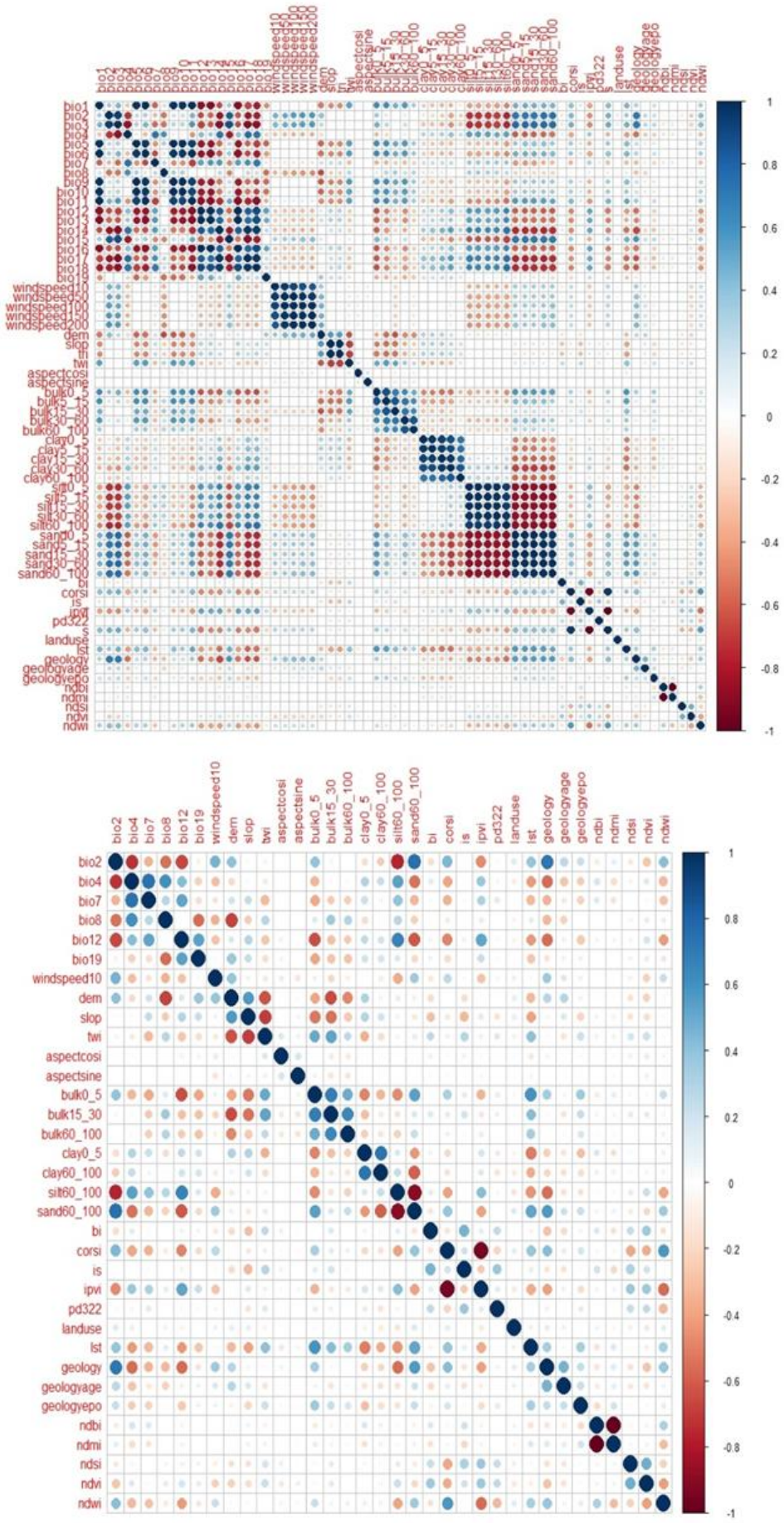

Fig. 3. Pearson's correlations test of the Predictor Variables

Table 1. List of predictive variables used in modeling areas with homogeneous potential for spring presence

Category		Variable name	Description	Abbreviation	Units	Spring
Bioclimatic*		Annual Mean temperature	The monthly average temperature	BIO 1	(◦C)	Reject
		Mean diurnal temperature	Average monthly (max temp – min temp)	BIO 2	(◦C)	Accept
		Isothermality	(BIO2/BIO7) (×100)	BIO 3	Percent	Reject
		Temperature seasonality	The amount of annual temperature variation calculated from the standard deviation of monthly temperature averages×100	BIO 4	(◦C)	Accept
		Maximum temperature of the warmest month	The highest monthly temperature that has been recorded in a certain year	BIO 5	(◦C)	Reject
		Minimum Temperature of the Coldest Month	The occurrence of the lowest monthly temperature in a given year	BIO 6	(◦C)	Reject
		Temperature Annual Range	Temperature variation over a given period (BIO5-BIO6)	BIO 7	(◦C)	Accept
		Mean temperature of the wettest quarter	The average temperatures experienced during the wettest quarter	BIO 8	(◦C)	Accept
		Mean temperature of the driest quarter	The average temperatures experienced during the driest quarter	BIO 9	(◦C)	Reject
		Mean temperature of the warmest quarter	The average temperatures experienced during the hottest quarter	BIO 10	(◦C)	Reject
		Mean temperature of the coldest quarter	The average temperatures in the coldest quarter	BIO 11	(◦C)	Reject
		Annual precipitation	This is the sum of all total monthly precipitation values	BIO 12	mm	Accept
		Precipitation of the wettest month	The total amount of precipitation experienced in the wettest month	BIO 13	mm	Reject
		Precipitation of the driest month	The total amount of precipitation experienced in the driest month	BIO 14	mm	Reject
		Precipitation seasonality	The monthly total precipitation standard deviation from the monthly total precipitation means	BIO 15	Percent	Reject
		Precipitation of the wettest quarter	The total amount of precipitation experienced during the wettest quarter	BIO 16	mm	Reject
		Precipitation of the driest quarter	The overall amount of precipitation experienced during the driest quarter	BIO 17	mm	Reject
		Precipitation of the warmest quarter	The total amount of precipitation that falls during the hottest	BIO 18	mm	Reject
		Precipitation of the Coldest Quarter	The total amount of precipitation experienced during the coldest quarter	BIO 19	mm	Reject
Wind**		windspeed	windspeed10m		m/s	Accept
			Windspeed50m		m/s	Reject
			windspeed100m		m/s	Reject
			windspeed150m		m/s	Reject
			Windspeed200m		m/s	Reject
Physical properties	Physical properties	Bulk density	Bulk density in depth 0-5 centimeter	Bulk 0-5	cg/cm^3	Accept
		Bulk density	Bulk density in depth 5-15 centimeter	Bulk 5-15	cg/cm^3	Reject
		Bulk density	Bulk density in depth 15-30 centimeter	Bulk 15-30	cg/cm^3	Accept
		Bulk density	Bulk density in depth 30-60 centimeter	Bulk 30-60	cg/cm^3	Reject
		Bulk density	Bulk density in depth 60-100 centimeter	Bulk 60-100	cg/cm^3	Accept
		Sand	Sand in depth 0-5 centimeter	Sand 0-5	g/kg	Reject
		Sand	Sand in depth 5-15 centimeter	Sand 5-15	g/kg	Reject
		Sand	Sand in depth 15-30 centimeter	Sand 15-30	g/kg	Reject
		Sand	Sand in depth 30-60 centimeter	Sand 30-60	g/kg	Reject
		Sand	Sand in depth 30-60 centimeter	Sand 60-100	g/kg	Accept
		Silt	Silt in depth 0-5 centimeter	Silt 0-5	g/kg	Reject
		Silt	Silt in depth 5-15 centimeter	Silt 5-15	g/kg	Reject
		Silt	Silt in depth 15-30 centimeter	Silt 15-30	g/kg	Reject
		Silt	Silt in depth 30-60 centimeter	Silt 30-560	g/kg	Reject
		Silt	Silt in depth 60-100 centimeter	Silt 60-100	g/kg	Accept
		Clay content	Clay content in depth 0-5 centimeter	Clay 0-5	g/kg	Accept
		Clay content	Clay content in depth 5-15 centimeter	Clay 5-15	g/kg	Reject
		Clay content	Clay content in depth 15-30 centimeter	Clay 15-30	g/kg	Reject
		Clay content	Clay content in depth 30-60 centimeter	Clay 30-60	g/kg	Reject
		Clay content	Clay content in depth 60-100 centimeter	Clay 60-100	g/kg	Accept
Edaphic**		index	S	Salinity	Unitless	Reject
			IS	Salinity Index	Unitless	Accept
			NDSI	Normalized Difference Salinity Index	Unitless	Accept

		BI	Brightness Index	Unitless	Accept
		PD322	Potential Different	Unitless	Accept
		IPVI	Infrared Percentage Vegetation Index	Unitless	Accept
		CRSI	Canopy Response Salinity Index	Unitless	Accept
Landuse**	landuse	landuse		Unitless	Accept
Lst**	lst	lst	Land Surface Temperature	Unitless	Accept
Geology***	geology	geologyepoch		Unitless	Accept
		geologyage		Unitless	Accept
		geology		Unitless	Accept
Vegetation**	index	NDVI	Normalized Differential Vegetation Index	Unitless	Accept
	index	NDBI	Normalized Differential Built-up Index	Unitless	Accept
Hydrologic**	index	NDMI	Normalized Differential Moisture Index	Unitless	Accept
		NDWI	Normalized Differential water Index	Unitless	Accept
Topographic***	Altitude	Altitude above sea level (obtained from optical sensors ASTER satellite, 90 m)	DEM	m	Accept
	TWI	Topographic wetness index (Produced from DEM)	TWI	Unitless	Accept
	TRI	Terrain Ruggedness Index	TRI	Unitless	Reject
	Slope	Percent change in that elevation over a certain distance	Slope	Degree	Accept
	Aspect Cosine	Aspect Cosine (Derived from DEM)	Aspectcosi	Degree	Accept
	Aspect Sine	Aspect Sine (Derived from DEM)	Aspectsine	Degree	Accept

* https://www.worldclim.org
** https://globalsolaratlas.info/download/iran
*** https://soilgrids.org/
**** Google Earth Engine
*****Iran Geological Organization
****** www.earthexplorer.usgs.gov

2.4. Modeling the distribution of areas with homogeneous potential for spring presence

This study employed ten algorithms from the Biomod2 software package (Thuiller et al., 2009) to model areas likely to have spring presence. Table 2 provide a summary of the models used from the BioMod 2 software package. Additionally, the BioMod software package was utilized to generate absence points. In the modeling process, 70% of presence points were used to build the models, while 30% were reserved for performance evaluation of the models. Moreover, to enhance modeling accuracy, five repetitions were considered.

In this study, the accuracy of the models was evaluated using three statistical coefficients. The first method involved assessing the ROC rate. The Receiver Operating Characteristic (ROC) curve is a graphical technique used to evaluate a model's performance in predicting the presence or absence of groundwater sources (springs) based on relevant environmental factors (Fielding and Bell, 1997). The second method entails calculating the True Skill Statistic (TSS), which is used with presence-absence models. TSS serves as a valuable indicator for interpreting real ecological phenomena. Studies have shown a high correlation between ROC and TSS. As a result, in studies where the findings are presented as presence-absence maps, TSS can be an appropriate alternative to ROC (Walther et al., 2002).

Cohen's Kappa evaluates the level of agreement between two assessors who have separately classify N cases into C distinct categories. The earliest use of statistics similar to Kappa can be traced back to Galton and Smeeton (Smeeton, 1985; Galton, 1892). ROC, Kappa, and TSS values less than 0.5 indicate poor performance in the model. Values ranging from 0.5 to 0.6 represent very weak agreement, while values between 0.6 and 0.7 indicate weak agreement. Values between 0.7 and 0.8 indicate moderate agreement, between 0.8 and 0.9 reflect good agreement, and values from 0.9 to 1 represent high agreement in the modeling (Yi et al., 2016; Swets, 1988).

Table 2. List of models used from the BioMod 2 software package

Abbreviation	Full name	References
GLM	Generalized Liner Model	Austin et al.,1984
GBM	Generalized Boosting Method	Austin et al.,1984
CTA	Classification Tree Analysis	Hastie et al.,1994
ANN	Artificial Neural Network	Breiman et al.,1984
SRE	Surface Range Envelope	Harrell et al.,1996
FDA	Flexible Denotative Analysis	Nix, 1986
MARS	Multivariate Adaptive Regression Spline	Hastie et al., 1994
RF	Random Forest	Friedman., 1991
MaxEnt	Maximum entropy model	Elith and Franklin., 2013
ESMs	Techniques and their ensembles	Damaneh et al., 2022

Furthermore, to obtain a geographical perspective of the areas that have suitable climatic and environmental conditions for the existence of springs in the study area, maps highlighting regions prone to spring occurrence have been consistently created. The map of susceptible areas is generated using Support Vector Machine (SVM) models, with values ranging from 0 to 1000. Zero indicates the lowest probability, while 1000 represents the highest probability. To enhance the understanding of the distribution, the map was classified into four categories using the Natural Breaks (Jenks) algorithm in ArcGIS 10.8 software. The categories are as follows: areas with no potential for spring occurrence (0 to 250), areas with low potential (250 to 500), areas with moderate potential (500 to 750), and areas highly susceptible to spring occurrence (750 to 1000).

3. Results and Discussion

Identifying areas with high potential for groundwater using spring data is a crucial method for conserving and effectively managing freshwater resources, particularly in semi-arid regions. Therefore, machine learning algorithms and remote sensing have gained popularity in this field.

Many studies have focused on assessing groundwater potential by applying machine learning algorithms and utilizing natural factors obtained from remote sensing (RS). However, the conditional parameters for each region, influenced by topography and other environmental factors, are specific to that area. Table 3 presents the values of the KAPPA, TSS, and ROC indices, which are key and commonly used metrics for identifying areas with similar potential. The modeling process in the majority of the models used in this study shows that they have achieved a good to moderate level of agreement. had the highest accuracy rates, The performance analysis of models for determining areas with similar potential for spring existence in terms of their accuracy metrics reveals that the Random Forest (RF) model achieved highest accuracy rates, with 81.6%, 81.4%, and 96.9% for the KAPPA, TSS, and ROC parameters, respectively.

By comparing these ten models, the random forest (RF) model demonstrated the highest accuracy, while the ESMs model ranked second. Conversely, the SRE model exhibited lower performance compared to the other ten models. The evaluation of inter-rater reliability through KAPPA values revealed a strong correlation among all ten models. This suggests that the models exhibit higher compatibility when measuring a constant phenomenon (Landis and Koch, 1977).

Therefore, based on the results and values presented in Table 3, the random forest (RF) model will be selected as the preferred model and will serve as the basis further calculations. Table 3 highlights the highest accuracy values and key variables that influence the

distribution of areas with comparable potential for spring presence. Finally, the ensemble model and chosen models will be used to present the results.

Table 3. Advanced Machine Learning Algorithms (MLA) performance statistics

Accuracy Parameter	GLM	GBM	GAM	CTA	ANN	SRE	FDA	MARS	RF	MAXENT	ESMs
KAPPA	0.734	0.756	0.736	0.754	0.699	0.374	0.752	0.738	0.816	0.738	0.789
TSS	0.733	0.753	0.735	0.752	0.698	0.379	0.751	0.737	0.814	0.737	0.789
ROC	0.937	0.941	0.938	0.918	0.899	0.689	0.939	0.936	0.969	0.938	0.968

The percentage of relative importance of environmental variables in modeling areas with potential spring presence is depicted in Figure 4 – A. Upon closer examination of Figure 4 – A, it becomes evident that the most significant environmental variables in the Random Forest method are the topographic factors (Altitude above sea level, Topographic wetness index, Slope), climatic factors (BIO7, BIO19, BIO12), and soil factors (Sand 60-100 cm, Silt 60-100 cm, Clay 0-5 cm, Land Surface Temperature), which had the greatest impact on the geographical distribution of areas with potential spring presence.

The relative importance analysis of all environmental factors in the ensemble model indicates that climatic factors (BIO7, BIO19, BIO2, BIO12), topographic factors (Altitude above sea level, Topographic wetness index, Slope), and soil factors (Sand 60-100 cm, Silt 60-100 cm, Clay 60-100 cm, Land Surface Temperature) Play a crucial role in the geographical distribution of areas susceptible to spring presence in eastern and northeastern Iran as shown in Figure 4 – B.

A

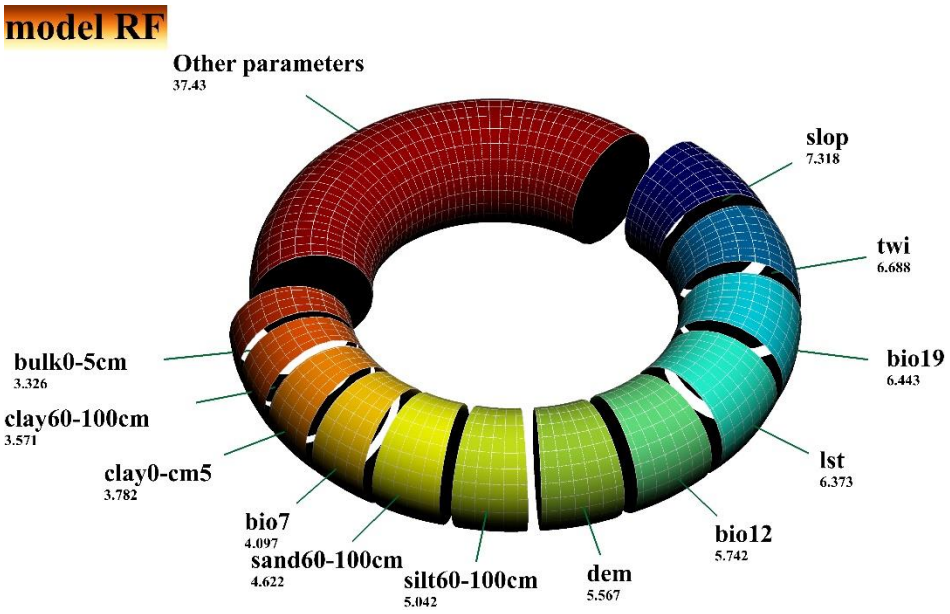

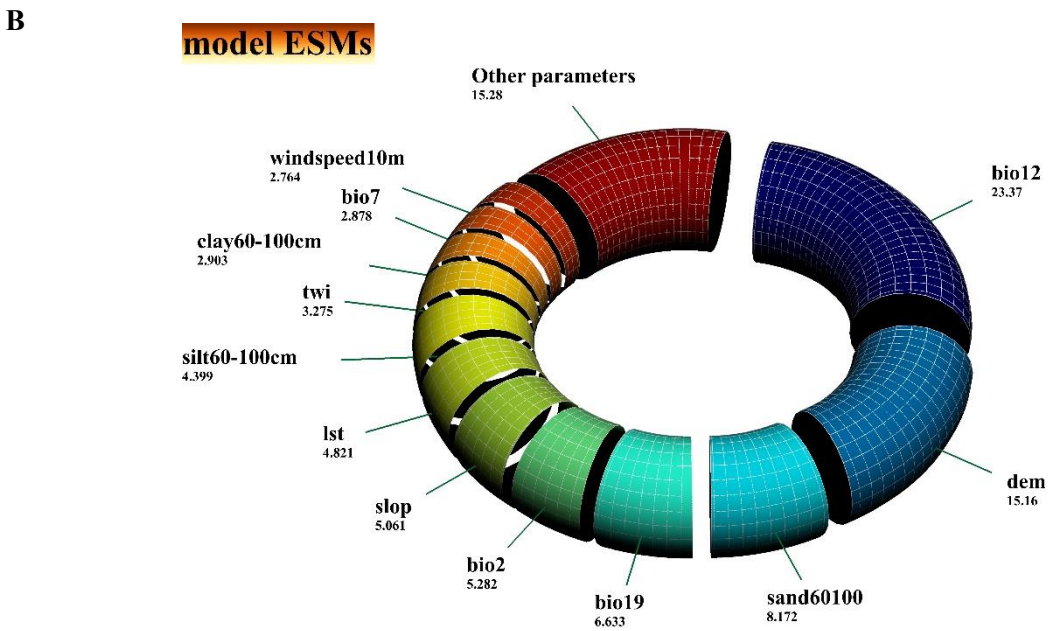

Fig. 4. Percentage of relative importance of influential environmental parameters in determining areas with groundwater potential. (A) Chosen random forest model (B) Ensemble model

As shown in Table 4, the chosen RF and ESMs models exhibit an area between 38,077 to 43,993 square kilometers, equivalent to 13.04% to 15.07% of the studied areas. These findings indicate high to very high potential for the presence or revitalization of groundwater resources (springs), demonstrating the areas with the greatest geographical distribution where springs are likely to successfully establish or exist. The percentage Distribution of Each Class of Groundwater Potential Maps in Modeling of Eastern and Northeastern Iran is depicted in Figure 5.

Table 4. Area and Percentage of Areas with Groundwater Potential in Modeling of Eastern and Northeastern Iran

Class	Chosen model ESMs		Chosen model RF	
	Area (Km^2)	Area (%)	Area (Km^2)	Area (%)
Low	224663	76.94	242412	83.01
Moderate	23336	7.99	11522	3.95
High	20983	7.19	10475	3.59
Very High	23010	7.88	27602	9.45

Overall, according to Figure 6, it becomes apparent that without proper and serious planning, the study area will experience a decrease and loss of these water resources.

This will lead to increased migration, higher unemployment, and the disappearance of industries and agriculture in the region (Statistical Center of Iran).

This study investigated groundwater potential in eastern and northeastern Iran by employing a comprehensive suite of 66 environmental variables and comparing the performance of ten advanced machine learning algorithms. The findings indicated that the Random Forest (RF) model consistently outperformed other algorithms (GLM, GBM, CTA, ANN, SRE, FDA, MARS, MaxEnt, and ESMs) based on KAPPA (0.816), TSS (0.814), and ROC (0.969) indices, suggesting its superior ability to accurately predict areas with high spring potential in the study region. The high accuracy of the RF model aligns with findings from several recent studies focused on groundwater potential mapping.

For instance, Naghibi et al. (2017), Golkarian et al. (2018), Moghaddam et al. (2020), and Ahmed Khan and Jhamnani (2023) reported RF as yielding prominent results in similar hydrogeological settings. This agreement could be attributed to RF's inherent strengths in handling complex, non-linear relationships and high-dimensional datasets without significant overfitting, as noted by Caruana et al. (2006) and Naghibi et al. (2019).

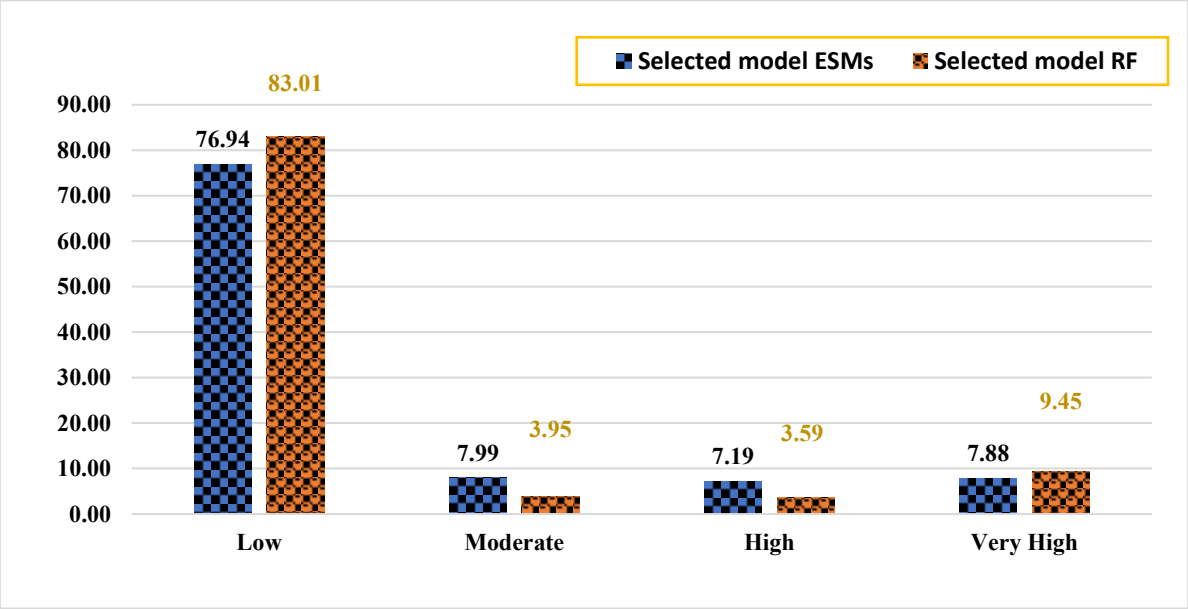

Fig. 5. Percentage Distribution of Each Class of Groundwater Potential Maps in Modeling of Eastern and Northeastern Iran

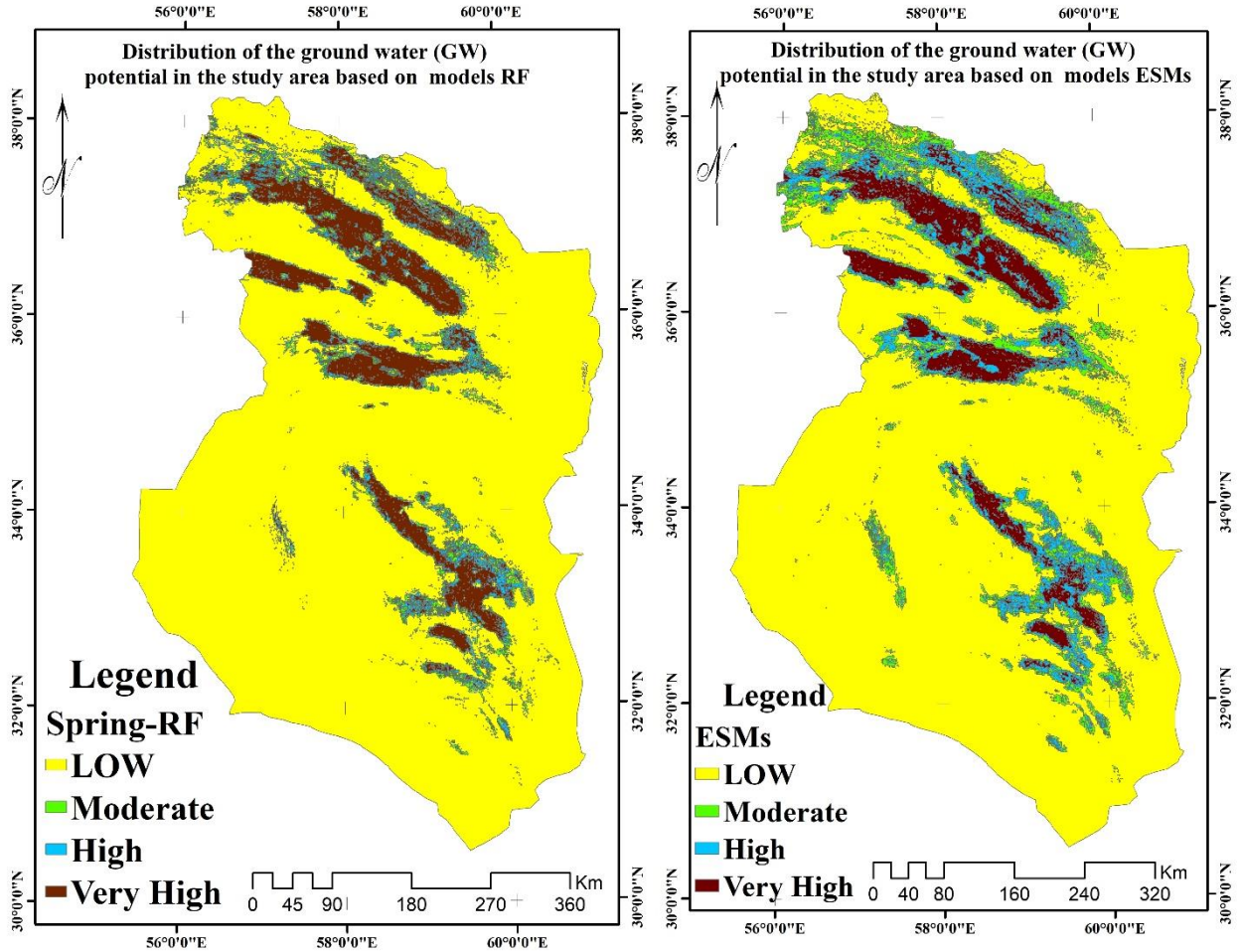

Fig. 6. Distribution of Groundwater Potential (GW) in the Study Area Based on Chosen Random Forest and Ensemble Models

The analysis of variable importance in the RF model revealed that topographic factors (Altitude, TWI, Slope), climatic factors (BIO7, BIO19, BIO12), and soil factors (Sand 60-100 cm, Silt 60-100 cm, Clay 0-5 cm, Land Surface Temperature) were the most influential in determining spring potential. This finding partially contrasts with studies by Naghibi et al. (2016), Chen et al. (2019), and Prasad et al.

(2020), which highlighted the significance of NDVI and drainage density.

This discrepancy could be due to the specific environmental characteristics of the study area in eastern and northeastern Iran, where topographic and specific climatic/soil conditions might exert a more dominant control on spring occurrence compared to vegetation cover or surface drainage patterns. The relatively arid to semi-arid climate of the region, as described in the Methodology, might reduce the direct influence of vegetation indices in comparison with factors directly affecting water accumulation and infiltration. Furthermore, the results revealed that the Terrain Ruggedness Index (TRI) had minimal contribution aligns with Kalantar et al. (2019) and Pradhan et al. (2021), suggesting that while topography plays a role (as evidenced by Altitude and Slope), extreme ruggedness might not be a primary determinant for spring locations in this specific geographical context.

The ensemble model (ESMs) also demonstrated high performance, ranking second to RF. This underscores the potential benefit of combining multiple modeling approaches to leverage their individual strengths and potentially improve predictive robustness, as suggested by Damaneh et al. (2022). The lower performance of the Surface Range Envelope (SRE) model might be attributed to its simpler approach, which may not effectively capture the complex environmental gradients influencing groundwater potential in the study area. The spatial distribution of high to very high groundwater potential zones, as predicted by the RF and ESMs models, identified areas covering 13.04% to 15.07% of the study region. These findings provide valuable insights for water resource management and conservation efforts in eastern and northeastern Iran, highlighting areas where focused investigation and sustainable exploitation strategies could be most effective.

The projected decrease and loss of water resources in the region without proper planning, as indicated by the Statistical Center of Iran, further emphasizes the urgency and importance of these findings for regional sustainability.

Despite the robust methodology and insightful results, this study has several limitations that should be considered when interpreting the findings. Firstly, the availability of spring location data, while substantial (7,355 points), is inherently biased towards known and accessible springs. There might be other unrecorded or less accessible springs whose environmental characteristics are not fully captured in our training data. This could potentially affect the generalizability of the models to predict spring potential in completely uninvestigated areas. Secondly, while we incorporated a comprehensive set of environmental variables, the spatial resolution of some datasets (e.g., 1000x1000 meters) might not fully capture the fine-scale heterogeneity of certain environmental factors that could influence spring occurrence. Higher resolution data, if available, could potentially improve the accuracy and spatial specificity of the models.

Thirdly, the study assumes a static relationship between the environmental variables and spring occurrence at the time of data collection. Groundwater systems are dynamic, and long-term changes in climate, land use, and geological conditions could influence spring activity and potential over time. Incorporating temporal data and dynamic modeling approaches in future research could provide a more comprehensive understanding of groundwater potential under changing conditions. Fourthly, the selection of absence points as random background locations assumes that these points represent areas with no spring potential. While this is a common approach, it might not always be entirely accurate, as some background points could potentially have low or undiscovered spring potential.

Employing more informed strategies for selecting absence points, perhaps based on expert knowledge or specific hydrogeological criteria, could refine the model training. Finally, the validation of the models relied on statistical metrics (KAPPA, TSS, ROC) based on the presence-absence data. While these are standard and informative, further validation using independent hydrogeological data, such as spring discharge rates or aquifer characteristics, could provide a more direct assessment of the model's predictive capability in terms of actual groundwater availability.

Future research should focus on addressing these limitations. This could involve efforts to improve the comprehensiveness and spatial resolution of input data, incorporating temporal dynamics into the modeling process, exploring more sophisticated methods for selecting absence points, and validating the model predictions with independent hydrogeological datasets. Additionally, investigating the specific hydrological mechanisms linking the identified key environmental variables to spring occurrence could provide a deeper understanding of the underlying processes and further enhance the reliability of groundwater potential maps.

4. Conclusion

Effective and sustainable groundwater management remains a cornerstone of global water security and development, particularly in arid and semi-arid regions. However, in many developing nations, this objective is severely constrained by the lack of high-resolution hydrogeological data. Addressing this critical gap, the present study demonstrates the significant potential of Remote Sensing (RS)-based datasets combined with machine learning (ML) approaches to accurately assess groundwater potential, focusing on the eastern and northeastern regions of Iran, which are both climatically vulnerable and socio-economically reliant on groundwater resources.

This study employed eleven widely recognized ML algorithms and assessed their predictive performance using the Kappa coefficient, True Skill Statistic (TSS), and Receiver Operating Characteristic (ROC) metrics. The findings identified the Random Forest (RF) model and ensemble learning approaches as the most reliable predictors of spring occurrence, a critical proxy for groundwater availability. The RF model achieved an accuracy of 81.6%, delineating approximately 38,077 km² as having high to very high potential for spring occurrence, while the ensemble model identified 43,993 km². These spatially explicit maps are crucial for informing targeted water resource management strategies, including identifying optimal locations for watershed and aquifer recharge structures.

The study also highlighted the significant influence of various environmental and climatic factors on groundwater potential, including elevation, Topographic Wetness Index (TWI), slope, annual precipitation, mean annual temperature, temperature of the warmest month, soil texture (sand, silt, and clay content at a depth of 60–100 cm), and Land Surface Temperature (LST). Notably, the strong contribution of remote sensing (RS)-derived variables underscores their considerable value as a viable alternative to conventional ground-based measurements, particularly in data-scarce or inaccessible regions.

The integration of RS data with Digital Elevation Models (DEMs) presents a robust and scalable approach for comprehensive groundwater assessments. Furthermore, the integration of freely available machine learning algorithms implemented in the R statistical software, together with the Advanced Spaceborne Thermal Emission and Reflection Radiometer (ASTER) DEM enhances the cost-effectiveness, accessibility, and replicability of the proposed methodology.

While acknowledging limitations such as the scarcity of precise spring location data and detailed lithological information in some regions, the study recommends incorporating expert-driven methods, such as the Analytic Hierarchy Process (AHP), and employing indirect variables derived from DEMs and RS sources to mitigate these challenges. Ultimately, the adaptability of this framework to locally available datasets improves the robustness and transferability of groundwater potential mapping across diverse hydrogeological contexts, offering a valuable tool for advancing sustainable water resource management.

5. Data availability

Data sets generated and/or analyzed during the current study are not publicly available due to institutional rules, but they are available from the corresponding author upon reasonable request.

6. Disclosure statement

No potential conflict of interest was reported by the authors.

7. References

AlAyyash, S., Al-Fugara, A., Shatnawi, R., Al-Shabeeb, A. R., Al-Adamat, R., & Al-Amoush, H. (2023). Combination of metaheuristic optimization algorithms and machine learning methods for groundwater potential mapping. *Sustainability, 15*(3), 2499.

Al-Djazouli, M. O., Elmorabiti, K., Rahimi, A., Amellah, O., & Fadil, O. A. M. (2021). Delineating of groundwater potential zones based on remote sensing, GIS and analytical hierarchical process: A case of Waddai, eastern Chad. *GeoJournal, 86*(5), 1881–1894.

Al-Fugara, A., Pourghasemi, H. R., Al-Shabeeb, A. R., Habib, M., Al-Adamat, R., Al-Amoush, H., & Collins, A. L. (2020). A comparison of machine learning models for the mapping of groundwater spring potential. *Environmental Earth Sciences, 79*, 206.

Al-Kindi, K. M., & Janizadeh, S. (2022). Machine learning and hyperparameters algorithms for identifying groundwater aflaj potential mapping in semi-arid ecosystems using LiDAR, Sentinel-2, GIS data, and analysis. *Remote Sensing, 14*(21), 5425.

Arneth, A., Barbosa, H., Benton, T., Calvin, K., Calvo, E., Connors, S., Cowie, A., Davin, E., Denton, F., & van Diemen, R. (2019). Summary for policymakers. In P. R. Shukla, J. Skea, E. Calvo Buendia, V. Masson-Delmotte, H.-O. Pörtner, D. C. Roberts, P. Zhai, R. Slade, S. Connors, R. van Diemen, M. Ferrat, E. Haughey, S. Luz, S. Neogi, M. Pathak, J. Petzold, J. Portugal Pereira, P. Vyas, E. Huntley, K. Kissick, M. Belkacemi, & J. Malley (Eds.), *Climate change and land: An IPCC special report on climate change, desertification, land degradation, sustainable land management, food security, and greenhouse gas fluxes in terrestrial ecosystems* (ISBN 978-92-9169-154-8). Intergovernmental Panel on Climate Change (IPCC).

Arthur, J. D., Wood, H. A. R., Baker, A. E., Cichon, J. R., & Raines, G. L. (2007). Development and implementation of a Bayesian-based aquifer vulnerability assessment in Florida. *Natural Resources Research, 16*, 93–107.

Austin, M. P., Cunningham, R. B., & Fleming, P. M. (1984). New approaches to direct gradient analysis using environmental scalars and statistical curve-fitting procedures. *Vegetatio, 55*(1), 11–27.

Bhadani, V., Singh, A., Kumar, V., & Gaurav, K. (2023). Machine learning models to predict groundwater level in a semi-arid river catchment, Central India. In *EGU General Assembly*, Vienna, Austria.

Boughariou, E., Allouche, N., Ben Brahim, F., Nasri, G., & Bouri, S. (2021). Delineation of groundwater potentials of Sfax region, Tunisia, using fuzzy analytical hierarchy process, frequency ratio, and weights of evidence models. *Environment, Development and Sustainability, 23*(10), 14749–14774.

Breiman, L., Friedman, J., Olshen, R., & Stone, C. (1984). *Classification and regression trees*. Wadsworth International Group.

Caruana, R., & Niculescu-Mizil, A. (2006). An empirical comparison of supervised learning algorithms. In *Proceedings of the 23rd International Conference on Machine Learning (ICML '06)* (pp. 161–168). ACM.

Chen, W., Panahi, M., Khosravi, K., et al. (2019). Spatial prediction of groundwater potentiality using ANFIS ensembled with teaching-learning-based and biogeography-based optimization. *Journal of Hydrology, 572*, 435–448.

Chenini, I., Mammou, A. B., & May, M. E. (2010). Groundwater recharge zone mapping using GIS-based multi-criteria analysis: A case study in Central Tunisia (Maknassy Basin). *Water Resources Management, 24*, 921–939.

Chowdhury, A., Jha, M. K., Chowdary, V. M., & Mal, B. C. (2008). Integrated remote sensing and GIS-based approach for assessing groundwater potential in West Medinipur district, West Bengal, India. *International Journal of Remote Sensing, 30*(1), 231–250.

Corsini, A., Cervi, F., & Ronchetti, F. (2009). Weight of evidence and artificial neural networks for potential groundwater spring mapping: An application to the Mt. Modino area (Northern Apennines, Italy). *Geomorphology, 111*, 79–87.

Damaneh, J. M., Ahmadi, J., Rahmanian, S., Sadeghi, S. M. M., Nasiri, V., & Borz, S. A. (2022). Prediction of wild pistachio ecological niche using machine learning models. *Ecological Informatics, 69*, 101907.

DEP. (1993). *Carte hydrogeologique du Burkina Faso. Feuille Ouagadougou. Echelle 1:50000*. Ministère de l'Eau and Directorat Général de la Coopération au Développement, Pays-Bas.

Devanantham, A., Subbarayan, S., Singh, L., et al. (2020). GIS-based multi-criteria analysis for identification of potential groundwater recharge zones: A case study from Ponnaniyaru watershed, Tamil Nadu, India. *HydroResearch, 3*, 1–14.

Díaz-Alcaide, S., & Martínez-Santos, P. (2019). Advances in groundwater potential mapping. *Hydrogeology Journal, 27*, 2307–2324.

Eid, M. H., Elbagory, M., Tamma, A. A., Gad, M., Elsayed, S., Hussein, H., Moghanm, F. S., Omara, A. E.-D., Kovács, A., & Péter, S. (2023). Evaluation of groundwater quality for irrigation in deep aquifers using multiple graphical and indexing approaches supported with machine learning models and GIS techniques, Souf Valley, Algeria. *Water, 15*(1), 182.

Elbeih, S. F. (2015). An overview of integrated remote sensing and GIS for groundwater mapping in Egypt. *Ain Shams Engineering Journal, 6*(1), 1–15.

Elith, J., & Franklin, J. (2013). Species distribution modeling. In S. A. Levin (Ed.), *Encyclopedia of biodiversity* (2nd ed., pp. 692–705). Elsevier.

Falah, F., & Zeinivand, H. (2019). GIS-based groundwater potential mapping in Khorramabad in Lorestan, Iran, using frequency ratio (FR) and weights of evidence (WoE) models. *Water Resources, 46*(5), 679–692.

Fielding, A. H., & Bell, J. F. (1997). A review of methods for the assessment of prediction errors in conservation presence/absence models. *Environmental Conservation, 24*(1), 38–49.

Friedman, J. H. (1991). Multivariate adaptive regression splines. *The Annals of Statistics, 19*(1), 1–67.

Galton, F. (1892). *Finger prints*. Macmillan.

Ghayoumian, J., Mohseni Saravi, M., Feiznia, S., Nouri, B., & Malekian, A. (2007). Application of GIS techniques to determine areas most suitable for artificial groundwater recharge in a coastal aquifer in southern Iran. *Journal of Asian Earth Sciences, 30*(2), 364–374.

Golkarian, A., Naghibi, S. A., Kalantar, B., & Pradhan, B. (2018). Groundwater potential mapping using C5.0, random forest, and multivariate adaptive regression spline models in GIS. *Environmental Monitoring and Assessment, 190*(3), 149.

Grönwall, J., & Danert, K. (2020). Regarding groundwater and drinking water access through a human rights lens: Self-supply as a norm. *Water, 12*(2), 419.

Gupta, M., & Srivastava, P. K. (2010). Integrating GIS and remote sensing for identification of groundwater potential zones in the hilly terrain of Pavagarh, Gujarat, India. *Water International, 35*(2), 233–245.

Harrell, F. E., Jr., Lee, K. L., & Mark, D. B. (1996). Multivariable prognostic models: Issues in developing models, evaluating assumptions and adequacy, and measuring and reducing errors. *Statistics in Medicine, 15*(4), 361–387.

Hastie, T., Tibshirani, R., & Buja, A. (1994). Flexible discriminant analysis by optimal scoring. *Journal of the American Statistical Association, 89*(428), 1255–1270.

Jha, M. K., Chowdhury, A., Chowdary, V. M., & Peiffer, S. (2007). Groundwater management and development by integrated remote sensing and geographic information systems: Prospects and constraints. *Water Resources Management, 21*(2), 427–467.

Kalantar, B., Al-Najjar, H. A. H., Pradhan, B., Saeidi, V., Halin, A. A., Ueda, N., & Naghibi, S. A. (2019). Optimized conditioning factors using machine learning techniques for groundwater potential mapping. *Water, 11*(9), 1909.

Kamali Maskooni, E., Naghibi, S. A., Hashemi, H., & Berndtsson, R. (2020). Application of advanced machine learning algorithms to assess groundwater potential using remote sensing-derived data. *Remote Sensing, 12*(17), 2742.

Khan, Z. A., & Jhamnani, B. (2023). Identification of groundwater potential zones of Idukki district using remote sensing and GIS-based machine-learning approach. *Water Supply, 23*(6), 2426–2446.

Landis, J. R., & Koch, G. G. (1977). An application of hierarchical Kappa-type statistics in the assessment of majority agreement among multiple observers. *Biometrics, 33*(2), 363–374.

Lee, S., Song, K. Y., Kim, Y., & Park, I. (2012). Regional groundwater productivity potential mapping using a geographic information system (GIS)-based artificial neural network model. *Hydrogeology Journal, 20*(7), 1511–1527.

Magesh, N. S., Chandrasekar, N., & Soundranayagam, J. P. (2012). Delineation of groundwater potential zones in Theni district, Tamil Nadu, using remote sensing, GIS and MIF techniques. *Geoscience Frontiers, 3*(2), 189–196.

Martínez-Santos, P., & Renard, P. (2020). Mapping groundwater potential through an ensemble of big data methods. *Groundwater, 58*(4), 583–597.

Martínez-Santos, P., Díaz-Alcaide, S., De la Hera, A., & Gomez-Escalonilla, V. (2021). A multi-parametric supervised classification algorithm to map groundwater-dependent wetlands. *Journal of Hydrology, 603*(Part A), 126873.

Martín-Loeches, M., Reyes-López, J., Ramírez-Hernández, J., Temiño-Vela, J., & Martínez-Santos, P. (2018). Comparison of RS/GIS analysis with classic mapping approaches for siting low-yield boreholes for hand pumps in crystalline terrains: An application to rural communities of the Caimbambo province, Angola. *Journal of African Earth Sciences, 138*, 22–31.

Masoudi, R., Mousavi, S. R., Rahimabadi, P. D., Panahi, M., & Rahmani, A. (2023). Assessing data mining algorithms to predict the quality of groundwater resources for determining irrigation hazard. *Environmental Monitoring and Assessment, 195*(4), 319.

Mogaji, K. A., & Lim, H. S. (2018). Application of Dempster-Shafer theory of evidence model to geoelectric and hydraulic parameters for groundwater potential zonation. *NRIAG Journal of Astronomy and Geophysics, 7*(2), 134–148.

Moghaddam, D. D., Rahmati, O., Panahi, M., Tiefenbacher, J., Darabi, H., Haghizadeh, A., ... & Bui, D. T. (2020). The effect of sample size on different machine learning models for groundwater potential mapping in mountain bedrock aquifers. *Catena, 187*, 104421.

Mohammadi-Behzad, H. R., Charchi, A., Kalantari, N., Nejad, A. M., & Vardanjani, H. K. (2019). Delineation of groundwater potential zones using remote sensing (RS), geographical information system (GIS) and analytic hierarchy process (AHP) techniques: A case study in the Leylia–Keynow watershed, southwest of Iran. *Carbonates and Evaporites, 34*(4), 1307–1319.

Momeni Demaneh, J., Esmaeilpour, Y., Gholami, H., & Farashi, A. (2021). Properly predict the growth of (*Ferula assa-foetida* L.) in northeastern Iran using the maximum entropy model. *Journal of Range and Desert Research of Iran, 28*(3), 587–592.

Mumtaz, F., Li, J., Liu, Q., Tariq, A., Arshad, A., Dong, Y., Zhao, J., Bashir, B., Zhang, H., Gu, C., & Liu, C. (2023). Impacts of green fraction changes on surface temperature and carbon emissions: Comparison under forestation and urbanization reshaping scenarios. *Remote Sensing, 15*(3), 859.

Murthy, K. S. R., & Mamo, A. G. (2009). Multi-criteria decision evaluation in groundwater zones identification in Moyale-Teltele subbasin, South Ethiopia. *International Journal of Remote Sensing, 30*(11), 2729–2740.

Naghibi, S. A., Ahmadi, K., & Daneshi, A. (2017a). Application of support vector machine, random forest, and genetic algorithm optimized random forest models in groundwater potential mapping. *Water Resources Management, 31*(9), 2761–2775.

Naghibi, S. A., Moghaddam, D. D., Kalantar, B., Pradhan, B., & Kisi, O. (2017b). A comparative assessment of GIS-based data mining models and a novel ensemble model in groundwater well potential mapping. *Journal of Hydrology, 548*, 471–483.

Naghibi, S. A., Pourghasemi, H. R., & Dixon, B. (2016). GIS-based groundwater potential mapping using boosted regression tree, classification and regression tree, and random forest machine learning models in Iran. *Environmental Monitoring and Assessment, 188*(1), 44.

Naghibi, S. A., Dolatkordestani, M., Rezaei, A., Amouzegari, P., Heravi, M. T., Kalantar, B., & Pradhan, B. (2019). Application of rotation forest with decision trees as base classifier and a novel ensemble model in spatial modeling of groundwater potential. *Environmental Monitoring and Assessment, 191*, 1–20.

Nampak, H., Pradhan, B., & Manap, M. A. (2014). Application of GIS-based data driven evidential belief function model to predict groundwater potential zonation. *Journal of Hydrology, 513*, 283–300.

Nazir, J., Ali, M., Sarwar, A., Khan, S., Rehman, K., Fahim, B., & Iqbal, B. (2024). Delineation and validation of GIS-based groundwater potential zones under arid to semi-arid environment using multi-influence-factors approach. *Geology, Ecology, and Landscapes*, 1–17.

Nguyen, P. T., Ha, D. H., Avand, M., Jaafari, A., Nguyen, H. D., Al-Ansari, N., Van Phong, T., Sharma, R., Kumar, R., Le, H. V., Ho, L. S., Prakash, I., & Pham, B. T. (2020). Soft computing ensemble models based on logistic regression for groundwater potential mapping. *Applied Sciences, 10*(7), 2469.

Nix, H. A. (1986). A biogeographic analysis of Australian elapid snakes. *Atlas of Elapid Snakes of Australia, 7*, 4–15.

Obeidavi, S., Gandomkar, M., Akbarizadeh, G., & Delfan, H. (2021). Evaluation of groundwater potential using Dempster-Shafer model and sensitivity analysis of effective factors: A case study of North Khuzestan Province. *Remote Sensing Applications: Society and Environment, 22*, 100475.

Oh, H. J., Kim, Y. S., Choi, J. K., Park, E., & Lee, S. (2011). GIS mapping of regional probabilistic groundwater potential in the area of Pohang City, Korea. *Journal of Hydrology, 399*, 158–172.

Ozdemir, A. (2011). Using a binary logistic regression method and GIS for evaluating and mapping the groundwater spring potential in the Sultan Mountains (Aksehir, Turkey). *Journal of Hydrology, 405*, 123–136.

Panahi, M., Sadhasivam, N., Pourghasemi, H. R., Rezaie, F., & Lee, S. (2020). Spatial prediction of groundwater potential mapping based on convolutional neural network (CNN) and support vector regression (SVR). *Journal of Hydrology*. Pourtaghi, Z. S., & Pourghasemi, H. R. (2014). GIS-based groundwater spring potential assessment and mapping in the Birjand Township, southern Khorasan Province, Iran. *Hydrogeology Journal, 22*, 643–662.

Pradhan, A. M. S., Kim, Y. T., Shrestha, S., Huynh, T. C., & Nguyen, B. P. (2021). Application of deep neural network to capture groundwater potential zone in mountainous terrain, Nepal Himalaya. *Environmental Science and Pollution Research, 28*(15), 18501–18517.

Pradhan, B. (2013). A comparative study on the predictive ability of the decision tree, support vector machine, and neuro-fuzzy models in

landslide susceptibility mapping using GIS. *Computers & Geosciences, 51*, 350–365.

Prasad, P., Loveson, V. J., Kotha, M., & Yadav, R. (2020). Application of machine learning techniques in groundwater potential mapping along the west coast of India. *GIScience & Remote Sensing*, *57*(5), 735–752.

Seifu, T. K., Eshetu, K. D., Woldesenbet, T. A., Alemayehu, T., & Ayenew, T. (2023). Application of advanced machine learning algorithms and geospatial techniques for groundwater potential zone mapping in Gambela Plain, Ethiopia. *Hydrology Research*, *54*(10), 1246–1266.

Shah, S. H. I. A., Yan, J., Ullah, I., Aslam, B., Tariq, A., Zhang, L., & Mumtaz, F. (2021). Classification of aquifer vulnerability by using the DRASTIC index and geo-electrical techniques. *Water*, *13*(16), 2144.

Singh, L. K., Jha, M. K., & Chowdary, V. M. (2018). Assessing the accuracy of GIS-based multi-criteria decision analysis approaches for mapping groundwater potential. *Ecological Indicators*, *91*, 24–37.

Smeeton, N. C. (1985). Early history of the kappa statistic. *Biometrics*, *41*(3), 795–796.

Srivastava, P. K., & Bhattacharya, A. K. (2006). Groundwater assessment through an integrated approach using remote sensing, GIS and resistivity techniques: A case study from a hard rock terrain. *International Journal of Remote Sensing*, *27*(20), 4599–4620.

Swets, J. A. (1988). Measuring the accuracy of diagnostic systems. *Science*, *240*(4857), 1285–1293.

Tariq, A., & Shu, H. (2020). CA-Markov chain analysis of seasonal land surface temperature and land use land cover change using optical multi-temporal satellite data of Faisalabad, Pakistan. *Remote Sensing*, *12*(20), 3402.

Tariq, A., Yan, J., Gagnon, A. S., Riaz Khan, M., & Mumtaz, F. (2022). Mapping of cropland, cropping patterns and crop types by combining optical remote sensing images with decision tree classifier and random forest. *Geo-Spatial Information Science*, *26*(3), 302–320.

Thuiller, W., Lafourcade, B., Engler, R., & Araújo, M. B. (2009). BIOMOD – A platform for ensemble forecasting of species distributions. *Ecography*, *32*(3), 369–373.

Walther, G. R., Post, E., Convey, P., Menzel, A., Parmesan, C., Beebee, T. J. C., & Bairlein, F. (2002). Ecological responses to recent climate change. *Nature*, *416*(6879), 389–395.

Yi, Y. J., Cheng, X., Yang, Z. F., & Zhang, S. H. (2016). MaxEnt modeling for predicting the potential distribution of endangered medicinal plant (*H. riparia* Lour) in Yunnan, China. *Ecological Engineering*, *92*, 260–269.

Yu, H., Wen, X., Wu, M., Sheng, D., Wu, J., & Zhao, Y. (2022). Data-based groundwater quality estimation and uncertainty analysis for irrigation agriculture. *Agricultural Water Management*, *262*, 107423.

Zhang, X., Yuan, Y., Zhu, Z., Ma, Q., Yu, H., Li, M., Ma, J., Yi, S., He, X., & Sun, Y. (2021). Predicting the distribution of *Oxytropis ochrocephala* Bunge in the source region of the Yellow River (China) based on UAV sampling data and species distribution model. *Remote Sensing*, *13*(24), 5129.